Improved Data Association for ICP-based Scan Matching in Noisy and Dynamic Environments

Diego Rodriguez-Losada and Javier Minguez

Abstract— **This paper presents a technique to improve the data association in the Iterative Closest Point [1] based scan matching. The method is based on a distance-filter constructed on the basis of an analysis of the set of solutions produced by the associations in the sensor configuration space. This leads to a robust strategy to filter all the associations that do not explain the principal motion of the scan (due to noise in the sensor, large odometry errors, spurious, occlusions or dynamic features for example). The experimental results suggest that the improvement of the data association leads to more robust and faster methods in the presence of wrong correspondences.**

I. INTRODUCTION

A key issue in autonomous mobile robots is to keep track of the vehicle position. When the robot is equipped with range sensors, one common framework is scan matching. The objective is to compute the relative motion of a vehicle between two consecutive configurations using the sensor measurements. Although these techniques are local in nature, many applications in robotics such as mapping, localization or tracking incorporate them to estimate the relative robot displacement [2], [3], [4], [5], [6].

Scan matching is currently an active research area. Roughly, the existing techniques can be divided in two groups. The first one deals with structured scenarios [7], [8], [9] and the other with raw data [10], [11], [1]. The latter do not assume structure and estimates the sensor displacement by maximizing the overlap between the range measurements or scans. The most popular of these methods is the Iterative Closest Point (ICP) algorithm [1] (see [12] for variants of the original method). This method is based on an iterative process with two steps: First, a set of correspondent points between the scans is computed and then, the sensor displacement is estimated by minimizing the error of the correspondences. This process is repeated until convergence. Since no high level features are used, the computation of the joint matching of the points of both scans is computationally very expensive (exponential with the number of points of the scans). To reduce the complexity, the ICP-type algorithms use the nearest-neighbor rule to establish pairs of correspondences between the points of each scan.

More precisely, let a point $\mathbf{p} \in \mathbf{R}^2$ be defined by its two dimensional cartesian coordinates (p_x, p_y) and a sensor configuration $\mathbf{q} \in \mathbf{R}^2 \times [-\pi, \pi]$ by its position and orientation (x, y, θ). Let $d(\mathbf{p_1}, \mathbf{p_2})$ be a generic measurement of distance between two points. Most ICP algorithms use the Euclidean distance, but in [13] the authors show how other metrics can greatly improve the algorithm performance. Let be $\{\mathbf{p_1} \ldots \mathbf{p_{N_{ref}}}\}$ the points of reference scan Z_{ref} and $\{\mathbf{t_1} \ldots \mathbf{t_{N_{new}}}\}$ the points of the other scan Z_{new} (already expressed in the reference frame of Z_{ref}). For each iteration k, let $\mathbf{q_k}$ be the relative estimated transformation between both scans, with an initial value $\mathbf{q_0}$ (typically from odometry). Repeat:

1) For each $\mathbf{p_i}$ in Z_{ref} compute $\mathbf{r_i}$ as the closest point in Z_{new} (transformed to the system of reference Z_{ref} using the estimation $\mathbf{q_k}$):

$$\mathbf{r_i} = \arg \min_{\mathbf{t_j}} \{d(\mathbf{p_i}, \mathbf{t_j})\} \qquad (1)$$

The result is a set of N associations $A = \{(\mathbf{p_i}, \mathbf{r_i}) \mid i = 1 \ldots N\}$.

2) Compute the displacement estimation $\mathbf{q_{min}}$ that minimizes the mean square error between pairs of A:

$$\mathbf{q_{min}} = \arg \min_{\mathbf{q}} \sum_{\mathbf{i=1}}^{\mathbf{N}} \mathbf{d}(\mathbf{p_i}, \mathbf{q}(\mathbf{r_i}))^\mathbf{2} \qquad (2)$$

Let be $\mathbf{q_{sol}} = \mathbf{q_{min}} \oplus \mathbf{q_k}$, with $\oplus$ representing the composition of relative transformations [14]. If there is convergence the estimation is $\mathbf{q_{sol}}$, otherwise iterate again with $\mathbf{q_{k+1}} = \mathbf{q_{sol}}$.

Although existing ICP-based techniques work well in static environments [15], [16], [13], [17], their performance degrades in situations where the correspondence process becomes more difficult: (i) noise in the sensor, (ii) large errors in the sensor odometry, (iii) spurious, (iv) new discovered areas, (v) occlusions and (vi) dynamic obstacles, among others. This is because these working conditions affect the most critical point of the ICP: the establishment of the correspondences. This step is crucial for these techniques since the remaining steps of the strategy depend on their quality. The contribution of this paper is an improved data association to ameliorate the scan matching performance under the previous conditions.

Some works have addressed this difficulty by evaluating the correspondence error as a measure of its goodness. For instance, a trimmed version of the ICP [18] simply discards the worst correspondences in terms of distance. Other strategy is to split the scans in sectors and discard those with a high mean correspondence error [19]. In [20] and [6], the scan matching is formulated as a an Expectation-Maximization and the effect of dynamic

D. Rodriguez-Losada is with the Universidad Politécnica de Madrid, UPM, Spain. `diego.rlosada@upm.es`

J. Minguez is with the I3A and the University of Zaragoza, Spain. `jminguez@unizar.es`

measurements is minimized through a weighting process. Unfortunately, wrong correspondences do not always have a large correspondence error, which affects the robustness and the convergence of previous approaches.

In this paper we analyze the set of solutions produced by the ICP correspondences in the configuration space of the sensor to build a novel robust filtering strategy. The idea is to filter those associations that do not explain the main motion of the scan and thus are likely to be wrong associations. For this purpose, a coarse estimation of the transformation between the scans is first obtained, and then, it is used to check the correctness of each single association. In this way, associations that do not belong to a consensus set (the main motion of the scan) are culled, irrespective of their correspondence error. The experimental results suggest that the improvement of the data association leads to more robust and faster methods in the presence of wrong correspondences.

The paper is organized as follows: Sections II and III present the framework. In section IV, we discuss the experimental results and we compare our method with existing techniques. Finally we draw our conclusions in Section V.

II. ASSOCIATIONS IN THE SENSOR CONFIGURATION SPACE

Recall that we have a set $A = \{a_1 \ldots a_N\}$ of N associations. One association is $a_i = \{\mathbf{p_i}, \mathbf{r_i}\}$ such that $\mathbf{p_i} = (p_{ix}, p_{iy})$ and $\mathbf{r_i} = (r_{ix}, r_{iy})$. In the set A, p associations come from the *static structure*, m associations from the *dynamic obstacles* and d associations are *spurious* or *wrong*. In general $p > m + d$ (the static structure is predominant).

The proposed filtering strategy is based on the idea that if we had a coarse estimation of the correct solution, it could be used to test each single association and robustly discard wrong ones. This section introduces the properties of the associations in the sensor configuration space, as well as the tools required to perform this task.

A. Basic problem: 1 association

All possible sensor configurations $\mathbf{q} = (x, y, \theta)$ that solve one association $a = \{\mathbf{p}, \mathbf{r}\}$ (subindex i is omitted) hold:

$$\mathbf{p} = \mathbf{T} + \mathbf{R}(\theta)\mathbf{r} \qquad (3)$$

where $\mathbf{T} = (\mathbf{x}, \mathbf{y})$ is the sensor translation and $\mathbf{R}(\theta)$ is the rotation matrix. Equation (3) can be written as:

$$\mathbf{f}(x, y, \theta) = \mathbf{p} - (\mathbf{T} + \mathbf{R}(\theta)\mathbf{r}) \qquad (4)$$

Function $\mathbf{f}(x, y, \theta) = (0, 0)$ defines a one-dimensional manifold $\mathbf{h}(\theta)$ in the sensor configuration space $\mathbf{R}^2 \times [-\pi, \pi]$.

$$\mathbf{h}(\theta) = (p_x + ||\mathbf{r}|| \cos(\theta + \beta), p_y + ||\mathbf{r}|| \sin(\theta + \beta), \theta) \quad (5)$$

where $\beta = \arctan \frac{-r_y}{r_x}$. This manifold has the shape of a circular helix with center $\mathbf{p}$ and radius $||\mathbf{r}||$. Notice that the set of solutions $\mathbf{q}$ for each association is an helix (C^∞) in the sensor configuration space.

B. Distance from 1 association to a sensor configuration

Another tool that will be used later is the distance from a given sensor configuration $\mathbf{q_0} = (x_0, y_0, \theta_0)$ to an helix $\mathbf{h}(\theta)$ defined by an association. In the configuration space, we define the norm of $\mathbf{q}$ as in [13]:

$$||\mathbf{q}|| = \sqrt{x^2 + y^2 + L^2\theta^2} \qquad (6)$$

where L is a positive real number homogeneous to a length. We define the distance from a configuration to an helix:

$$d_{\mathbf{qh}}(\mathbf{q_0}, \mathbf{h}) = ||\mathbf{q_c} - \mathbf{q_0}||, \text{ such that } \mathbf{q_c} = \arg\min_{\mathbf{q} \in \mathbf{h}} ||\mathbf{q} - \mathbf{q_0}||^2 \qquad (7)$$

Since $\mathbf{h}(\theta)$ is a one dimensional manifold in θ (Equation (5)), the minimum of $||\mathbf{q} - \mathbf{q_0}||^2$ is given by:

$$\frac{\partial ||\mathbf{h}(\theta) - \mathbf{q_0}||^2}{\partial \theta} = 0 \qquad (8)$$

Developing we have an expression of the form:

$$a\theta + b\sin\theta + c\cos\theta + d = 0 \qquad (9)$$

where: $a = L^2$, $b = \mathbf{pr}^T - x_0 p_{2x} - y_0 p_{2y}$, $c = p_{1x}r_{2y} - p_{1y}r_{2x} - x_0 p_{2y} + y_0 p_{2x}$ and $d = -\theta_0 L^2$. Unfortunately there is no closed form solution for Equation (9) thus we linearize in $\theta \simeq \theta_l$:

$$\theta_{min} = \frac{(b\theta_l - c)\cos\theta_l - (c\theta_l + b)\sin\theta_l - d}{a + b\cos\theta_l - c\sin\theta_l} \qquad (10)$$

The linearization point is:

$$\theta_l = \arctan\frac{q_{0y} - p_y}{q_{0x} - p_x} - \arctan\frac{r_y}{r_x} \qquad (11)$$

computed as the projection of $\mathbf{q_0}$ to the cylinder that embeds the helix (Equation (5)). Substituting θ_{min} in Equation (5) we get $\mathbf{q_c}$. Finally:

$$d_{\mathbf{qh}}(\mathbf{q_0}, \mathbf{h})) = ||\mathbf{q_c} - \mathbf{q_0}|| \qquad (12)$$

C. Proximity of Manifolds to a Region of Reference

Let say that we have a region of configurations of reference defined like a compact set embedded in the configuration space $\Omega \in \mathbf{R}^2 \times [-\pi, \pi]$. One evaluation of the goodness of an association a is to compute the distance from its manifold $\mathbf{h}$ of solutions to this set:

$$d_{\Omega\mathbf{h}}(\Omega, \mathbf{h}) = d_{\mathbf{qh}}(\mathbf{q_c}, \mathbf{h}) \text{ such that } \mathbf{q_c} = \arg\min_{\mathbf{q} \in \Omega} d_{\mathbf{qh}}(\mathbf{q}, \mathbf{h}) \qquad (13)$$

where $d_{\mathbf{qh}}$ is the distance from a configuration to an helix. When the solution of reference is the motion of the sensor, then the distance of the manifolds that explain this motion to the solution is zero, while the other associations give a greater distance.

However, in realistic operation the measures are corrupted by noise. Although it is not described here in detail due to space constraints, one can use continuity arguments in Equation (13) to demonstrate that when the noise tends to zero, the solution tends to the perfect solution (zero distance). In any case, the noise degrades the solution and thus the location of the manifolds. By computing the distance of
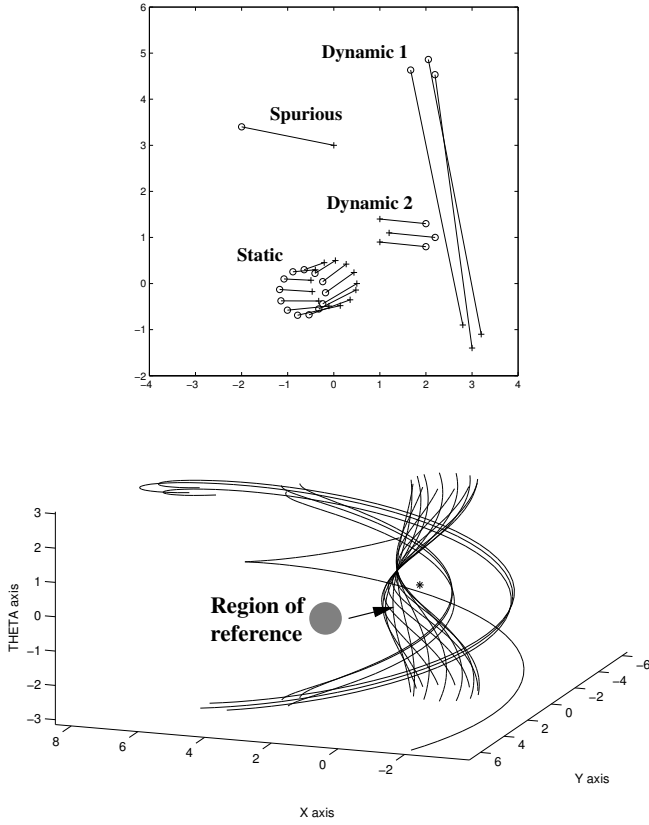
Fig. 1. This Figure shows a set of associations (top) and the curves that generate in the sensor configuration space (bottom). (Top) Two measurements with a given motion between them. The circle is static and there are two dynamic obstacles that have their motion plus the sensor motion. (Bottom) In the sensor configuration space, each association creates a curve of solutions. The *region of reference* is a set of configurations computed by a given method that explains the motion of the sensor. The curves closed to this set are created by associations of the static structure.
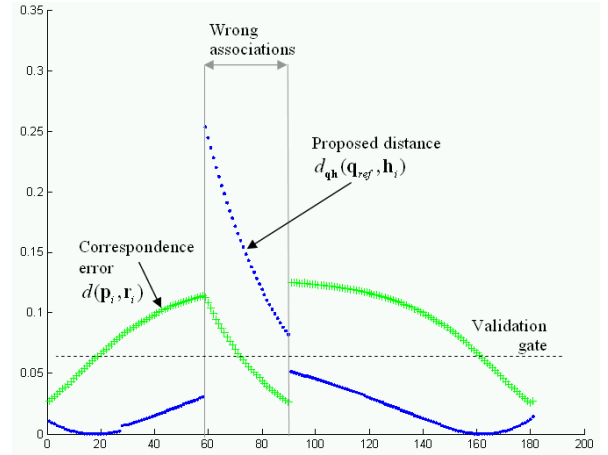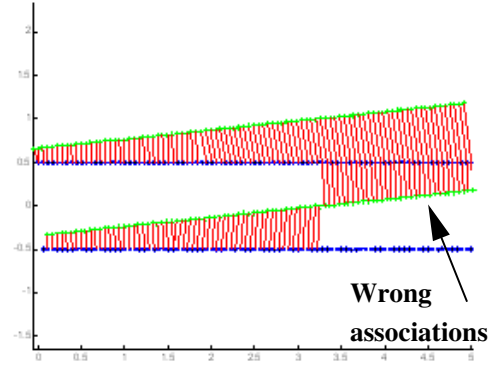
Fig. 2. (Top) Two scans from a corridor but translated and rotated, and the set A of nearest-neighbor associations with the distance [13]. (Bottom) Correspondence error $d(\mathbf{p_i}, \mathbf{r_i})$ (metric distance) and proposed distance $d_{\mathbf{qh}}(q_{ref}, h_i)$. The wrong associations are detected in the set $d_{\mathbf{qh}}(q_{ref}, h_i)$, while they cannot be robustly discarded based on the correspondence errors $d(\mathbf{p_i}, \mathbf{r_i})$.

the manifold to the solution of reference one have a robust criterion to deal with noise. Figure 1 shows an example.

This process is useful to evaluate associations if one can have in advance a good approximation of a region of configurations likely to explain the motion.

In summary, in this section we have described some properties of the associations in the configuration space and outlined one strategy to detect the static structure of the scenario based on the distance of the manifolds to a reference solution.

III. THE PROPOSED FRAMEWORK

In the previous section, we derived some tools to measure the distance from a given solution of reference to the set of solutions of each association. We show next how to use this distance to filter those associations likely to be incorrect. The resulting algorithm can be outlined as follows:

1) Search of correspondences. Equation (1) is used to obtain the initial set of associations A with a nearest neighbor approach.
2) Computation of the solution of reference. In this step we apply the least squares of Equation (2) with the

set A. The estimated solution is $\mathbf{q_{ref}}$ (solution of reference).
3) Filtering the associations. For all associations $a_i \in A$ we compute the $\overline{d_{\mathbf{qh}}(\mathbf{q_{ref}}, \mathbf{h_i})}$ as explained in subsection II-B. Then, those with high distance are filtered. The remaining set is A'.
4) Minimization. In this step we apply the least squares minimization of Equation (2) with the set A'.

The idea underlying this approach is that with the first minimization, we obtain a coarse estimation of the sensor displacement. In this process, all the correspondences take part. In the next step, we evaluate all the manifolds by computing their distance to the reference solution. If this distance is small, this means that the set of solutions of this association is closed to the solution of reference, and thus this association is likely to explain the same motion that the reference one. However, when the distance is large, the solution set is far from the reference solution. This means that this association comes from an spurious or wrong association and thus is rejected. At the end of this process we have a set A' of associations that explain a similar motion. Notice that A' is the set A but filtered with a criterion of

distance in the space of solutions.

We describe next an academic but illustrative example of this process. Figure 2(top) depicts two scans taken in a corridor, but one of them is translated and rotated. The nearest-neighbor strategy automatically process the associations computing the set A, with several incorrect correspondences. Figure 2(bottom) shows the distance between the correspondences (distance not processed in the Figure). Notice how using this distance criterion is difficult to find a validation gate.

In order to use the proposed strategy, we apply the minimization to compute an estimation of the displacement $\mathbf{q_{ref}}$. The solution $\mathbf{q_{ref}}$ is a coarse approximation of the motion (due to the large number of wrong associations). Then, we construct the validation gate for each association by computing the distance between the manifold of the association and $\mathbf{q_{ref}}$ (Equation 13). The distances are displayed in Figure 2(bottom), distance processed in the Figure. Low distances are right associations while wrong associations lead to distances significantly greater. In the limit, one could have a association $a_i = (\mathbf{p_i}, \mathbf{r_i})$ established between two overlapping points $\mathbf{p_i} = \mathbf{r_i}$, with a correspondence error $d(\mathbf{p_i}, \mathbf{r_i}) = 0$. It is basically impossible to filter this point with previous approaches, but not with our strategy since it could have a large value of $d_{\mathbf{qh}}(\mathbf{q_{ref}}, \mathbf{h_i}) > 0$.

IV. EXPERIMENTS

This section describes the experimental work developed to evaluate the filtering. As sensor, we used a SICK LMS200 mounted on a *B21r* robot. This sensor gathers 181 range measurements (with a field of view of $180°$) at 5Hz with a maximum range of 8.1m (we limited the range to 6m).

To check the influence of the filtering, we used the standard ICP and MbICP. However, we did not implement the refinements of the techniques described in [13] for both methods, since we wanted to study the effect of the filtering in the standard performance. We used the proposed filtering only in the standard MbICP implementation (that we refer to MbICP-IDA). Furthermore, the methodology is a little bit different from the one proposed in [13]. This is because in the context of the present paper the advantage might be in noisy scenarios. Thus, we artificially contamine all the points of the scans and inject outliers to test the methods. In fact, these conditions are more exigent in terms of noise than those described in [13].

In terms of inner parameters of the methods, we used a smooth criterion of convergence [16] that requires two consecutive iterations with a location correction lower than 0.0005 (m, rad) for each coordinate. The maximum number of iterations is 300. Furthermore, we set the maximum percentage of discarded associations to 20%.

We describe next the three types of experiments carried out: (i) static scenario, (ii) dynamic scenario and a (iii) a run in the laboratory.

A. Scan against scan experiments

In these experiment, we evaluated the scan matching performance with two data sets: (i) an static scenario artifi-
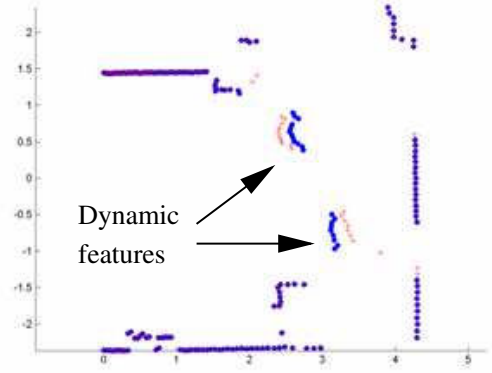

Fig. 3. Two range scans in a dynamic scenario.

cially corrupted with noise in the measurements and sensor displacement, and (ii) a dynamic scenario. The first dataset is composed by 879 laser scans acquired in a 60m trajectory along different kinds of scenarios: regular rooms, corridors, cluttered and open spaces, etc (Figure 4). Each scan is compared with itself, so ground truth is available $(0, 0, 0)$. To simulate sensor noise and outliers (reflections, occlusions, etc) each point is contaminated with uniformly distributed noise in the range ± 0.025m, and a random 10% of the points are also contaminated with noise in the range ± 0.50 m. For each scan 10 different initial random locations are generated (8790 runs for each range).

The second data set consists of 619 laser scans acquired in a fixed location with 2 or 3 people continuously walking in front of the robot (generating occlusions and non-static data points). Figure 3 shows an example. Each scan is compared with the next one, however, as the vehicle is static the ground truth is $(0, 0, 0)$. For each scan 10 different initial random locations are generated (6190 runs for each range).

The next two tables summarize the results.

TABLE I
MBICP +IDA VS MBICP AND ICP: NOISY STATIC SCENARIO

Static Scenario Noise ±0.025m 10% outliers	Method	ICP	MbICP	MbICP + IDA
	Conv. Rate (#)	23.73	20.9	14.51
Sensor error $(0.15m, 0.15m, 17°)$	Precision (m)	0.011	0.007	0.007
	Robustness (%)	98.01	99.60	99.93
	Conv. Rate (#)	32.09	27.46	19.24
Sensor error $(0.3m, 0.3m, 34°)$	Precision (m)	0.011	0.007	0.007
	Robustness (%)	92.67	95.90	99.17

We discuss first the results in terms of robustness. A run was considered a failure when the solution was larger than 0.02m in translation and 0.02rad in rotation (notice that the ground truth is $(0, 0, 0)$). These values are just a threshold used to identify failures of the method. In Table I we observe that all the methods are robust. However, as the noise in the sensor increases the robustness of the methods decreases. This effect also appears in the dynamic scenario since there are many issues involved like dynamic
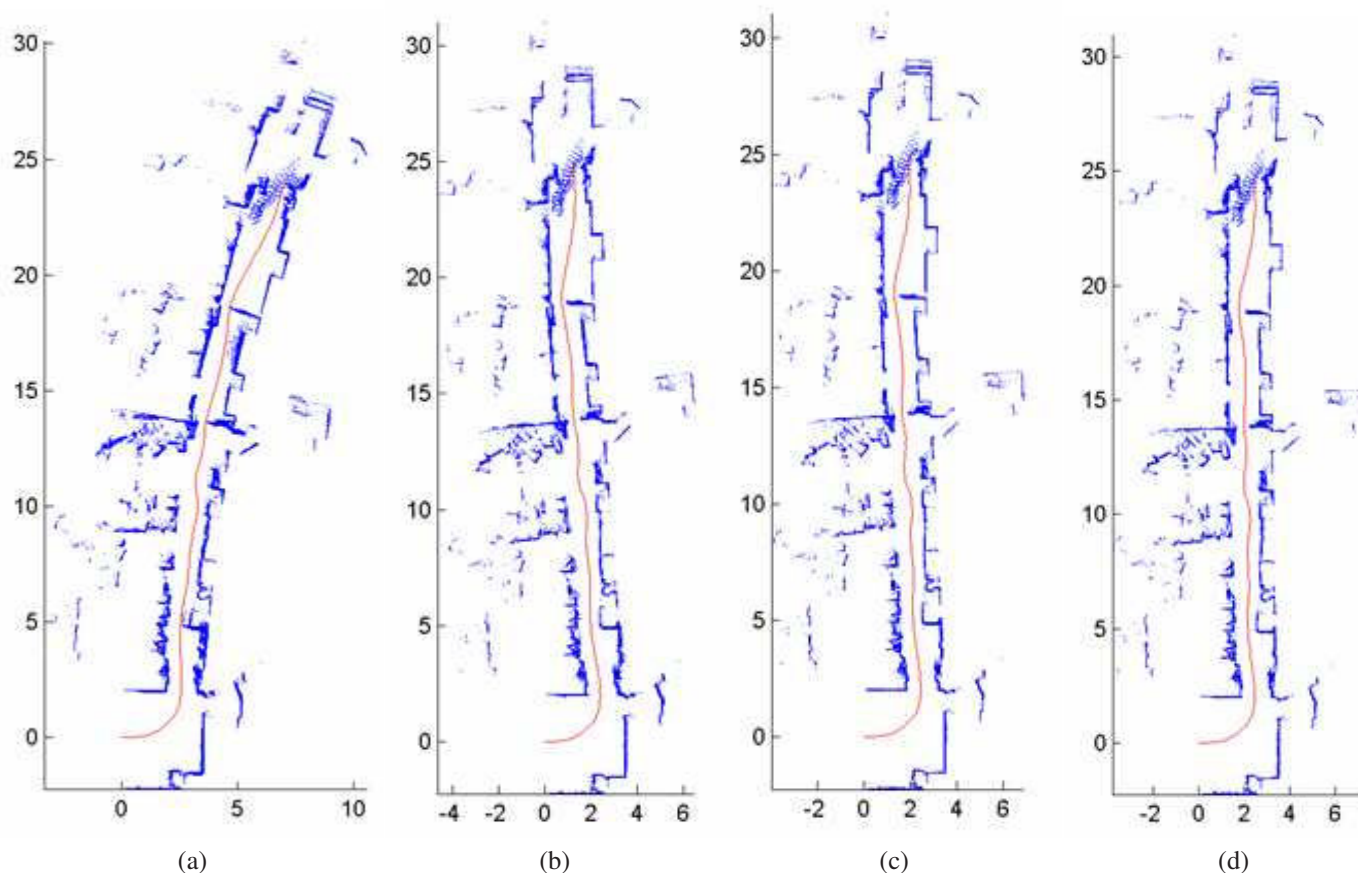
Fig. 4.   Visual odometry. (a) Odometry, (b) ICP, (c) MbICP and (d) MbICP+IDA.

TABLE II
MBICP +IDA VS MBICP AND ICP: DYNAMIC SCENARIO

Dynamic Scenario	Method	ICP	MbICP	MbICP + IDA
	Conv. Rate (#)	26.51	22.41	17.02
Sensor error	Precision (m)	0.024	0.004	0.004
$(0.15m, 0.15m, 17°)$	Robustness (%)	52.73	80.64	86.00
	Conv. Rate (#)	37.359	30.24	22.13
Sensor error	Precision (m)	0.025	0.004	0.004
$(0.3m, 0.3m, 34°)$	Robustness (%)	47.15	78.25	85.01

associations and occlusions affecting the correspondence step of the methods (see Table II). In any case, the filtered data association improves the robustness in both cases.

The MbICP and the MbICP+IDA have the same order of precision. This is because precision is very related with the behavior of the method in the vicinity of the solution. Since this analysis is performed for the runs that converged, then the role of the new data association is not very relevant (almost no error in the sensor location).

The MbICP+IDA converges faster than the other methods. This was expected since the new data association improves the correspondences and thus the subsequent minimization. The number of required iterations to converge is lower in all cases. Regarding the computation time, the time consumed

with the filter is not very significant (the profile of the code shows that more than 95% of the total computation time is used in the data association step).

In summary the MbICP with the filtering technique outperforms the standard methods in robustness, precision and convergence. This is because the proposed approach filters the incorrect data associations in the presence of large error locations, occlusions, dynamic objects, etc.

B. Visual map with scan matching

The second test corresponds to the matching of consecutive scans of the first data set. As the ground truth is not available, the validation is done by plotting all the scans using the locations estimated by the methods.

Figure 4 shows the maps obtained with the odometry and all the methods. However there is not a large difference between the maps. Only the map of the MbICP+IDA is slightly straighter than the map of the MbICP and the ICP. This is due to the filter used in the MbICP+IDA. The convergence rates (the average number of iterations) are 6.00, 6.06 and 6.14 for the MbICP+IDC, MbICP and ICP respectively. There is no a significant difference since the odometry is quite good.

We repeated the experiments by corrupting the sensor location with uniformly distributed noise in the range
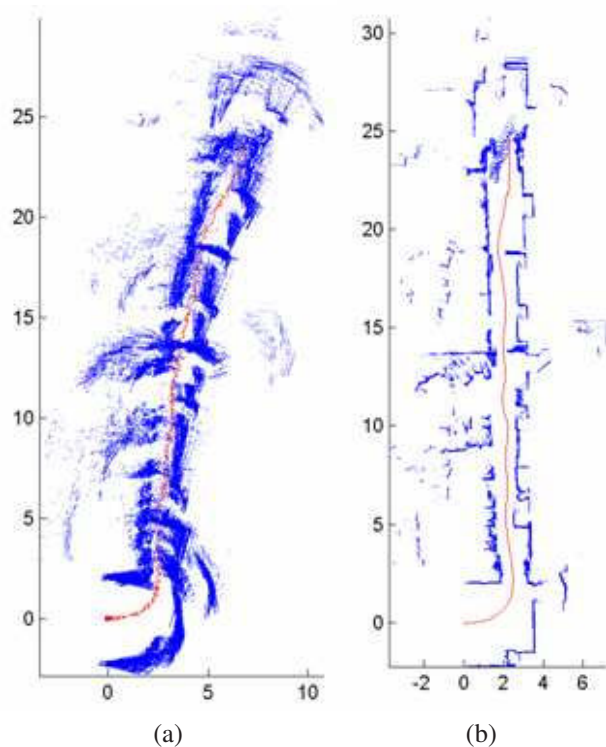
Fig. 5.   (a) Odometry, (b) MbICP+IDA.

$\pm(0.15m, 0.15m, 17°)$. Then the scan matching process is much more difficult since the working conditions are very noisy. Figure 5 shows the map of the odometry and the map with the odometry corrected with the MbICP-IDA. After many trials with the MbICP we found that the successful rate was very dependent on the parameters and the succesfull/failure rate result was not significant. However, the MbICP+IDA uses the filtering and achieves to map the scenario. The mean convergence rate was 19.86 which is slower than the other experiments. This is usual due to the iterations needed in the beginning to filter the spurious associations.

V. CONCLUSIONS

This paper presents a technique to improve the data association in the ICP-based scan matching. The method is based on a distance-filter constructed on the basis of an analysis of the set of solutions produced by the associations in the sensor configuration space. This leads to a robust strategy to filter all the associations that do not explain the principal motion of the scan, which greatly improves the next steps of the methods. The experimental results suggest that the improvement of the data association leads to a more robust and faster method in the presence of wrong correspondences.

Future work will concentrate in improving the rejection criterion with adaptive thresholds. Furthermore, we will investigate the usage of clustering strategies in the sensor configuration space of each pairing to explicitly classify scan points as static, dynamic, non-visible structure and outliers.

REFERENCES

[1] P.J. Besl and N.D. McKay, "A method for registration of 3-d shapes," *IEEE Transactions on Pattern Analysis and Machine Intelligence*, vol. 14, pp. 239–256, 1992.
[2] C.-C. Wang, C. Thorpe, and S. Thrun, "Online simultaneous localization and mapping with detection and tracking of moving objects: Theory and results from a ground vehicle in crowded urban areas," in *Proceedings of the IEEE International Conference on Robotics and Automation (ICRA)*, 2003.
[3] D. Hähnel, D. Fox, W. Burgard, and S. Thrun, "A highly efficient fastslam algorithm for generating cyclic maps of large-scale environments from raw laser range measurements," in *IEEE/RSJ International Conference on Intelligent Robots and Systems*, Las Vegas, Usa, 2003.
[4] L. Montesano, J. Minguez, and L. Montano, "Lessons learned in integration for sensor-based robot navigation systems," *International Journal of Advanced Robotic Systems*, vol. 3, no. 1, pp. 85–91, 2006.
[5] S. Lacroix, A. Mallet, D. Bonnafous, G. Bauzil, S. Fleury, M. Herrb, and R. Chatila, "Autonomous rover navigation on unknown terrains: Functions and integration," *International Journal of Robotics Research*, vol. 21, no. 10-11, pp. 917–942, Oct-Nov. 2002.
[6] L. Montesano, J. Minguez, and L. Montano, "Modeling the static and the dynamic parts of the environment to improve sensor-based navigation," in *IEEE International Conference on Robotics and Automation (ICRA)*, 2005.
[7] A. Grossmann and R. Poli, "Robust mobile robot localization from sparse and noisy proximetry readings using hough transform and probability grids," *Robotics and Autonomous Systems*, vol. 37, pp. 1–18, 2001.
[8] I.J. Cox, "Blanche: An experiment in guidance and navigation of an autonomous robot vehicle," *IEEE Transactions on Robotics and Automation*, vol. 7, pp. 193–204, 1991.
[9] J. A. Castellanos, J. D. Tardós, and J. Neira, "Constraint-based mobile robot localization," in *Advanced Robotics and Intelligent Systems*, IEE, Control Series 51, 1996.
[10] Peter Biber and Wolfgang Strafler, "The normal distributions transform: A new approach to laser scan matching," in *IEEE Int. Conf. on Intelligent Robots and Systems*, Las Vegas, USA, 2003.
[11] J. Gonzalez and R. Gutierrez, "Direct motion estimation from a range scan sequence," *Journal of Robotics Systems*, vol. 16, no. 2, pp. 73–80, 1999.
[12] S. Rusinkiewicz and M. Levoy, "Efficient variants of the icp algorithm," in *International Conference 3DIM*, 2001.
[13] J. Minguez, L. Montesano, and F. Lamiraux, "Metric-based iterative closest point scan matching for sensor displacement estimation," *IEEE Transactions on Robotics*, vol. 22, no. 5, pp. 1047 – 1054, 2006.
[14] R.Smith, M. Self, and P. Cheeseman, "Estimating uncertain spatial relationships in robotics," in *J.F. Lemmer AND L. N. Kanal*, D. Koditschek and J. Hollerbach, Eds., vol. 2. 1988.
[15] F. Lu and E. Milios, "Robot pose estimation in unknown environments by matching 2d range scans," *Intelligent and Robotic Systems*, vol. 18, pp. 249–275, 1997.
[16] S.T. Pfister, K.L. Kreichbaum, S.I. Roumeliotis, and J.W. Burdick, "Weighted range sensor matching algorithms for mobile robot displacement estimation," in *In Proceedings of the IEEE International Conference on Robotics and Automation (ICRA)*, 2002, pp. 1667–74.
[17] L. Montesano, J. Minguez, and L. Montano, "Probabilistic scan matching for motion estimation in unstructured environments," in *IEEE Int. Conf. on Intelligent Robots and Systems (IROS)*, 2005.
[18] D. Cheverikov, D. Svirko, and P. Krsek, "The trimmed iterative closest point algorithm," in *International Conference on Pattern Recognition*, 2002, vol. 3, pp. 545–548.
[19] O. Bengtsson and A-J. Baerveldt, "Localization in changing environments by matching laser range scans," in *EURobot*, 1999, pp. 169–176.
[20] B. Jensen and R. Siegwart, "Scan alignment with probabilistic distance metric," in *Proc. of the IEEE-RSJ Int. Conf. on Intelligent Robots and Systems*, Sendai, Japan, 2004.